

# INTERNATIONAL SOCIETY FOR SOIL MECHANICS AND GEOTECHNICAL ENGINEERING



*This paper was downloaded from the Online Library of the International Society for Soil Mechanics and Geotechnical Engineering (ISSMGE). The library is available here:*

<https://www.issmge.org/publications/online-library>

*This is an open-access database that archives thousands of papers published under the Auspices of the ISSMGE and maintained by the Innovation and Development Committee of ISSMGE.*

*The paper was published in the proceedings of the 10th International Conference on Physical Modelling in Geotechnics and was edited by Moonkyung Chung, Sung-Ryul Kim, Nam-Ryong Kim, Tae-Hyuk Kwon, Heon-Joon Park, Seong-Bae Jo and Jae-Hyun Kim. The conference was held in Daejeon, South Korea from September 19<sup>th</sup> to September 23<sup>rd</sup> 2022.*

## Centrifuge test to assess $K_0$ in unsaturated soil layers with varying groundwater table levels

M.M. Turner, O. Komolafe & M. Ghayoomi

*Department of Civil & Environment Engineering, University of New Hampshire, USA*

K. Ueda & R. Uzuoka

*Disaster Prevention & Research Institute, Kyoto University, Japan*

**ABSTRACT:** Lateral earth pressure analyses typically assume backfill soil is either in the fully saturated or dry state. However, backfill material is commonly in an unsaturated condition, especially when soil is located above the groundwater table or compacted. In this region, matric suction generates apparent cohesion altering the soil strength. This paper presents the results of a centrifuge experiment to determine the influence of the degree of saturation on the at-rest coefficient of lateral earth pressure,  $K_0$ . The experimental program consisted of an initially fully saturated soil specimen. Then, the water table elevation was gradually lowered, in flight, while the change in  $K_0$  was recorded. For soil with unsaturated layers present, findings suggest  $K_0$  decreases with a reduction in degree of saturation due to a reduction in soil unit weight and an introduction of matric suction.

**Keywords:** Centrifuge modelling, lateral earth pressure, unsaturated soil, water table depth

### 1 INTRODUCTION

For the design of many geotechnical structures, the state of stress in the soil is a primary analysis parameter. To design these structures, both vertical and horizontal (lateral) earth pressure must be estimated. Vertical earth pressure can be simply estimated based on the unit weight and depth of the soil. Meanwhile, the lateral earth pressure depends on several factors, including strain, shear strength, unit weight, and drainage conditions. When a mass of soil has experienced zero lateral strain, the soil is known to be in the at-rest condition. In this condition, the at-rest coefficient of earth pressure,  $K_0$ , is used to estimate the lateral earth pressure acting on a structure by a soil mass. Estimation of  $K_0$  has been the subject of much research over the years, often by using empirical correlations. Jaky (1944) proposed an estimation of  $K_0$  for normally consolidated sands, as a function of effective friction angle. For clays, researchers have correlated  $K_0$  with plasticity index (Alpan 1967; Massarsch 1979) or plasticity index and overconsolidation ratio (Brooker and Ireland 1965). Most of these studies have focused on determining  $K_0$  for soils in the dry or fully saturated states. However, many geotechnical structures are built on, or embedded in, unsaturated soils. Unsaturated soils are widespread in zones above the groundwater table where capillary rise leads to the introduction of a three-phase material (composed of solids, water, and air). In these regions, the unit weight of the soil is influenced by the degree of

saturation, while the shear strength of the soil increases compared to the fully saturated condition due to the introduction of negative pore water pressure (matric suction) (Fredlund et al. 1996). Matric suction acts as an apparent cohesion and pulls the soil particles together.

In this study, a centrifuge test was performed to investigate the influence of the water table depth on  $K_0$  in a sandy silt.  $K_0$  for unsaturated soil is determined according to the definition by Lu & Likos (2004), shown in Equation 1(a) and for saturated soil according to Equation 1(b).

$$K_0 = \frac{\sigma_h - u_a}{\sigma_v - u_a} \quad \text{for } S < 1.0 \quad (1a)$$

$$K_0 = \frac{\sigma_h - u_w}{\sigma_v - u_w} \quad \text{for } S = 1.0 \quad (1b)$$

where  $\sigma_h$  and  $\sigma_v$  are the total stresses generated in the vertical and horizontal directions, respectively.  $S$  is the degree of saturation of the soil. While  $u_a$  and  $u_w$  are the pore air and water pressure, respectively.  $\sigma_h$  was measured directly during the experiments using miniature earth pressure transducers while  $\sigma_v$  was estimated based on the depth of the water table below the soil surface and the corresponding influence of the degree of saturation on the unit weight.  $u_w$  was estimated based on the depth of the earth pressure transducer below the water table depth and  $u_a$  was assumed to be zero as the soil layer was open to the atmosphere throughout testing. Where necessary, Equation 2 (Jaky 1944) is employed to estimate the value

of  $K_0$  for saturated soils based on the effective friction angle of the normally consolidated soil,  $\phi'$ .

$$K_0 = 1 - \sin\phi' \quad (2)$$

$K_0$  was also estimated for unsaturated soils based on Poisson's ratio,  $\mu$ , as implemented by Komolafe and Ghayoomi (2021), and shown in Equation 3. The degree of saturation-dependent function for Poisson's ratio of unsaturated soils by Thota et al. (2021) was used in this equation.  $K_0$  values estimated using Equation 3 are compared to those determined experimentally, thus highlighting the potential use of Equation 3.

$$K_0 = \frac{\mu}{1 - \mu} \quad (3)$$

The centrifuge test was started with an initially fully saturated soil layer. Then, the water table depth was gradually lowered in-flight while the change in  $\sigma_h$  was recorded.

## 2 EXPERIMENTAL CONDITIONS

The experiment was performed using the geotechnical centrifuge located at the Disaster Prevention Research Institute of Kyoto University. Samples were prepared in a laminar container of length and width equal to 50 and 20 cm, respectively. The soil material used in this experimental campaign was a manufactured silica sand, known under the commercial name of Silica Sand No. 9. This material is classified as sandy silt under the United Soil Classification System and has a specific gravity of 2.72. The Soil Water Retention Curve (SWRC) of this soil, fitted with the van Genuchten (1980) model is shown in Fig. 1. According to Fig. 1, the air entry matric suction and  $S_r$  of this soil are about 7.6 kPa and 19%, respectively. Models were prepared in a 1 g environment by dry pluviating the material from a pre-defined drop height into an impermeable membrane installed inside the laminar container. The soil was prepared in uniform 20 mm lifts with pluviating terminated after reaching the desired depth of the sample layer equal to 205 mm. This sample preparation method produced a soil with an initial dry density of about  $1463 \text{ kg/m}^3$  and void ratio of about 0.81. After preparing the sample, the soil layer was saturated by allowing de-aired water to flow through valves located at the base of the laminar container. The hydraulic gradient between the water supply tank and the soil layer was carefully monitored to avoid piping throughout the specimen. After the water table reached the surface of the soil layer, the saturation process was terminated.

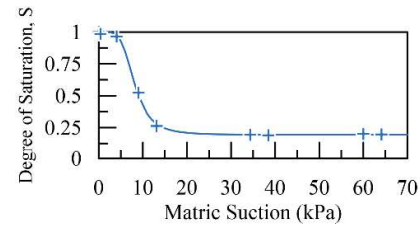


Fig. 1. Soil water retention curve (SWRC) of the sandy silt.

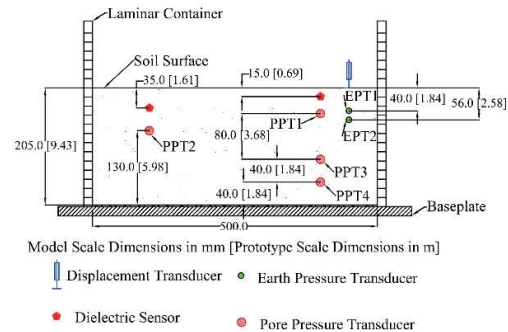


Fig. 2. Schematic layout of the centrifuge test, showing initial conditions.

Throughout the sample preparation process, instruments were installed at select locations in the soil layer according to the longitudinal view of the experimental layout given in Fig. 2. Instruments included laser displacement sensors, moisture probes, pore pressure transducers (PPTs), and earth pressure transducers (EPTs). One laser displacement sensor was used to measure the model surface settlement throughout the experiments. Two EPTs were mounted to the longitudinal wall of the laminar container and were arranged to measure the horizontal earth pressure of the soil in the at-rest condition at depths of 40 and 56 mm. Four PPTs were installed at depths of 45, 75, 125, and 165 mm to measure the water table depth throughout testing. Finally, moisture sensor probes were used to estimate the volumetric water content of the soil at depths of 15 and 35 mm.

After preparing the soil layer, the laminar box was transferred to the centrifuge platform and the centrifuge was spun-up to 46 g centripetal acceleration. According to the centrifuge scaling laws presented by Wood (2004) and the abovementioned g-level, a prototype soil layer of thickness 9.4 m was simulated. After reaching the target g-level, the surface settlement was monitored until the change in settlement became negligible. At this point, the height of the water table above the surface of the soil layer was estimated using the PPTs and was found to be about 0.36 m (prototype scale). The soil was in the fully saturated condition and lateral pressure data was obtained by the EPTs for about 3 hours in the prototype scale. Next, the water table depth was gradually lowered

in-flight while the change in  $\sigma_h$  was recorded. The following procedure, implemented by Borghei et al. (2020) and Turner et al. (2021), was used to lower the water table and gather data: (1) water was allowed to drain from the specimen by remotely opening the valves (previously used to saturate the specimen); (2) the valves were closed after a short period and drained water was routed to an onboard storage tank; (3) PPTs were used to estimate the depth of the water table in the soil; (4) EPT data was collected for a short period; and (5) steps 1-4 were repeated until the water table reached a depth of about 3.64 m below the soil surface.

### 3 RESULTS AND DISCUSSION

Results are presented to highlight the influence of the water table depth and degree of saturation on  $K_0$ . Throughout the analysis, corrections for sensor locations and soil density have been made to consider surface settlements. The following results are presented in the prototype scale.

#### 3.1 Pore Pressures

Fig. 3 shows the pore pressure values measured throughout the experiment, plotted with respect to time. Significant reductions in measured pore pressures correspond to reductions in the water table elevation in the soil profile. For this analysis, the data corresponding to ten distinct water table elevations were selected and analyzed. Time durations of pore pressure data used to determine the water table depths are highlighted in Fig. 3 (pore pressure data was averaged along these time spans). Estimated water table depths are given in Table 1, along with the names used to reference the water table depth. A negative water table elevation indicates the water level was above the surface of the soil layer and the soil was in the fully saturated condition.

#### 3.2 Earth Pressures

Fig. 4 highlights the EPT data plotted with respect to time.  $\sigma_h$  were averaged along the same time intervals used to estimate the water table depths. The measured  $\sigma_h$  data for WL1 (fully saturated layer) can be used to validate the sensor measurements.  $\sigma_h$  data for WL1 can be compared to estimated  $\sigma_h$  calculated considering the saturated unit weight of the soil, water table depth, sensor depth, and  $K_0$  calculated using Equation 2 ( $\phi' = 38^\circ$ ). According to Fig. 5, the measured values of  $\sigma_h$  closely match the estimated ones. Therefore, measured values were accepted as accurate and used throughout the analysis. It should be noted that, although minor, the differences between measured and estimated values are expected to be associated with the size of the EPT sensors (0.5 m diameter). Considering lateral earth pressure is influenced by depth, the size of the sensor may have influenced the results.

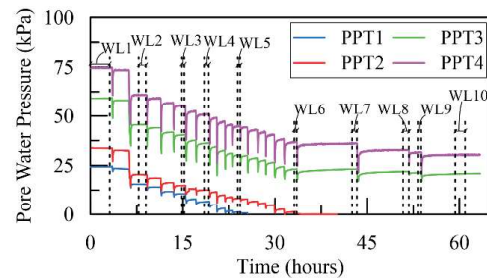


Fig. 3. Measured pore water pressure throughout the test along with the time durations used to estimate the water table depths.

Table 1. Water table depths and identifiers.

| Water Table Name | Water Table Depth Below Soil Surface (m) | Water Table Name | Water Table Depth Below Soil Surface (m) |
|------------------|--|------------------|--|
| WL1              | -0.365                                   | WL6              | 2.813                                    |
| WL2              | 0.918                                    | WL7              | 2.965                                    |
| WL3              | 1.463                                    | WL8              | 3.323                                    |
| WL4              | 1.632                                    | WL9              | 3.434                                    |
| WL5              | 2.041                                    | WL10             | 3.638                                    |

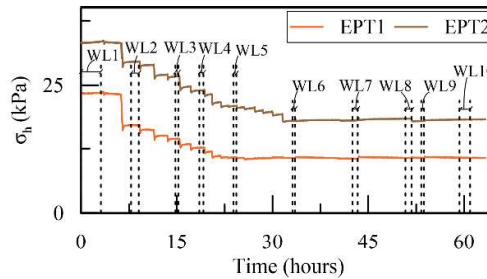


Fig. 4. Measured earth pressure during the test along with time durations used to estimate the average earth pressures.

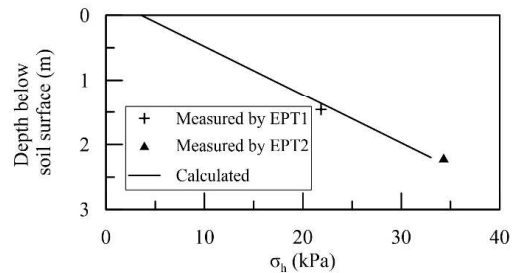


Fig. 5. Comparison of measured versus estimated values of  $\sigma_h$  for WL1 as a function of EPT depth below the soil surface.

#### 3.3 $K_0$ for Unsaturated Soils

The values of  $K_0$  at the depths of the EPTs were calculated according to Equation 1. To calculate  $K_0$ , the value of  $\sigma_v$  at the EPT depths were estimated from the total unit weight of the soil ( $\gamma_t$ ) and depth below the soil surface. Above and below the water table elevation, the  $\gamma_t$  of the soil can be correlated to the degree of saturation of the soil through the SWRC shown in Fig. 1, with matric suctions calculated assuming hydrostatic

conditions. Fig. 6 shows  $\gamma_t$  calculated at specific depths throughout the soil layer across each water table elevation. These curves were used to evaluate  $\sigma_v$  at the depth of the EPTs, and hence  $K_0$ .

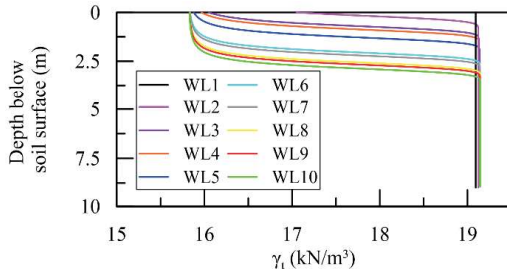


Fig. 6. Variation of  $\gamma_t$  with respect to soil depth below the soil layer surface.

Values of  $K_0$  are displayed as a function of the degree of saturation of the soil at the depth of the corresponding EPT in Fig. 7.  $K_0$  values are shown only when unsaturated and saturated soils are present above the depth of the EPT (i.e., results from WL1 are not shown). According to the figure,  $K_0$  varies with  $S$ .  $K_0$  reduces from a maximum value of about 0.61 at  $S = 1.0$  to a minimum value of about 0.47 as the soil approaches  $S_r$ . The reduction of  $K_0$  values with  $S$  can be explained due to a reduction in  $\gamma_t$  throughout the soil profile and an introduction of matric suction. As  $S$  nears  $S_r$ , the contribution of capillary effect on matric suction becomes negligible and  $\gamma_t$  has a greater influence on the behavior. Finally, the values of  $K_0$  obtained from Equation 3 are similar to those found experimentally.

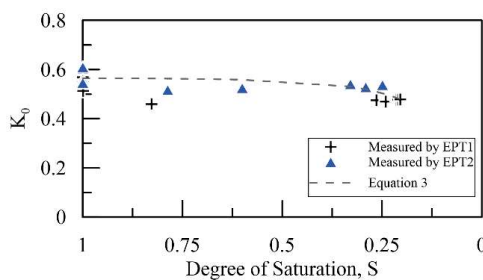


Fig. 7.  $K_0$  versus  $S$  when both saturated and unsaturated soil layers are present above the EPT depth.

#### 4 CONCLUSIONS

A centrifuge experiment was performed to investigate the influence of the degree of saturation on  $K_0$ . The model was fully saturated; then, the water table depth was gradually lowered in-flight while changes in  $\sigma_h$  were recorded using EPTs located at two depths below the soil layer surface. For soil with unsaturated

and saturated layers present, findings suggest that the value of  $K_0$  decreases with reduced degree of saturation. Finally, this study confirms the applicability of correlating  $K_0$  with  $\mu$  to predict lateral earth pressure in unsaturated soils, provided the SWRC and the  $\mu$  of the soil in the dry and fully saturated states are known.

#### ACKNOWLEDGEMENTS

This study was partly supported by the collaborative research program (2019W-03) of the Disaster Prevention Research Institute of Kyoto University and the Institute of International Education Global E3 program.

#### REFERENCES

- Alpan, I. 1967. The Empirical Evaluation of the Coefficient  $K_0$  and  $K_{OR}$ . *Soils and Foundations*, 7(1): 31–40. <https://doi.org/10.3208/sandf1960.7.31>
- Borghesi, A., Ghayoomi, M., & Turner, M. 2020. Effects of Groundwater Level on Seismic Response of Soil Foundation Systems. *Journal of Geotechnical and Geoenvironmental Engineering*, 146(10): 04020110. [https://doi.org/10.1061/\(ASCE\)GT.1943-5606.0002359](https://doi.org/10.1061/(ASCE)GT.1943-5606.0002359)
- Brooker, E. W., & Ireland, H. O. 1965. Earth Pressures at Rest Related to Stress History. *Canadian Geotechnical J.*, 2: 1–15.
- Fredlund, D. G., Xing, A., Fredlund, M. D., & Barbour, S. L. 1996. *The relationship of the unsaturated soil shear strength to the soil-water characteristic curve*. Canadian Geotechnical Journal, 33(3): 440–448. <https://doi.org/10.1139/t96-065>
- Jaky, J. 1944. The coefficient of earth pressure at rest. *Journal of the Hungarian Society of Architects and Eng.*, 25: 355–358.
- Komolafe, O., & Ghayoomi, M. 2021. Theoretical Ultimate Lateral Resistance Near the Soil Surface in Unsaturated Cohesionless Soils. *46th Annual Conference on Deep Foundations*: 178–187.
- Lu, N., & Likos, W. J. 2004. *Unsaturated Soil Mechanics*. Wiley.
- Massarsch, K. R. 1979. Lateral Earth Pressure in Normally Consolidated Clay. *7th European Conference on Soil Mechanics and Foundation Engineering*, 2: 245–249.
- Thota, S. K., Cao, T. D., & Vahedifard, F. 2021. Poisson's Ratio Characteristic Curve of Unsaturated Soils. *Journal of Geotechnical and Geoenvironmental Engineering*, 147(1): 04020149. [https://doi.org/10.1061/\(ASCE\)GT.1943-5606.0002424](https://doi.org/10.1061/(ASCE)GT.1943-5606.0002424)
- Turner, M. M., Ghayoomi, M., Ueda, K., & Uzuoka, R. 2021. Performance of rocking foundations on unsaturated soil layers with variable groundwater levels. *Géotechnique*, 1–14. <https://doi.org/10.1680/jgeot.20.P.221>
- van Genuchten, M. 1980. A Closed-form Equation for Predicting the Hydraulic Conductivity of Unsaturated Soils. *Soil Science Society of America Journal*, 44(5): 892–898. <https://doi.org/10.2136/sssaj1980.03615995004400050002x>
- Wood, D. M. 2004. *Geotechnical Modelling*. CRC Press.